Research Article | Vol. 12, No. 10 / 1 Oct 2022 / Optical Materials Express 4088
Optical Materials EXPRESS

Anti-reflection coatings for epsilon-near-zero materials

LAURA C. WYNNE,[1,*] CISSY ZHANG,[1] USENOBONG AKPAN,[1] ANDREA DI FALCO,[1] AND SEBASTIAN A. SCHULZ[1,2]

[1] University of St Andrews, Department of Physics and Astronomy, N. Haugh, St. Andrews KY16 9SS, United Kingdom
[2] sas35@st-andrews.ac.uk
[*] lw207@st-andrews.ac.uk

Abstract: Epsilon-near-zero (ENZ) materials have attracted much interest within the photonics community due to the various novel light-matter interactions that can occur in the ENZ regime. These materials display a large impedance mismatch between the ENZ material and free space, making it difficult to couple light into the medium at normal incidence. In this article, we demonstrate that enhanced light coupling into an ENZ metamaterial stack can be achieved via the design and fabrication of anti-reflection coatings, which are simple to fabricate via e-beam evaporation. The coating fabricated has been optimized not only to minimize reflection but also aims to maximize transmission — making these designs applicable to e.g. beam shaping applications. We achieve a transmission enhancement of 20% through our metamaterial over a 150 nm range and reflection minimization of 50% over a 200 nm range.

1. Introduction

Epsilon-Near-Zero (ENZ) materials have attracted much attention for both linear and nonlinear optical applications [1], such as enhanced harmonic generation [2], strong nonlinear index shifts [3,4], phase matching free nonlinear processes [5,6], wavefront shaping [7], enhanced directive emission [8] or coupling through arbitrary apertures [9]. Their potential is further increased by the ENZ property being available in a wide range of materials and at a wide range of wavelengths, e.g. through tuning of the plasma frequency in transition metal oxides [10], control of structural dimensions in integrated photonics structures [11] and metal-dielectric multilayer structures [12,13].

However, the main limitation in their utilization in various applications is the high impedance mismatch with free space and conventional materials, which prevents optimal light coupling into an ENZ film. Thus the transmission and nonlinear effects are limited, while a large fraction of the incident field is simply reflected at the surface of the ENZ metamaterial. Approaches for solving this include tuning the angular incidence to enhance the internal field through the electromagnetic boundary conditions requiring a continuous tangential field at a material interface or coupling between antenna arrays and the ENZ medium. While tuning the angular incidence is effective at enhancing nonlinear effects [3] it is strongly polarisation dependent and results in strongly angle dependent behaviour. Similarly, antenna coupling has been successfully used to enhance the nonlinear response of ENZ films [14]. However, this approach is complex and costly, requiring electron beam lithography to define the nanostructures antenna array and the observed optical response is not that of either the antenna or the underlying ENZ film, but a coupled complex optical resonance system [15,16] . Yet, for conventional optical materials, the control of transmission and reflection is a solved problem and routinely achieved via thin films acting as either a high-reflection or anti-reflection (AR) coating.

#469382 https://doi.org/10.1364/OME.469382
Journal © 2022 Received 1 Jul 2022; revised 6 Sep 2022; accepted 6 Sep 2022; published 21 Sep 2022

Optical Materials EXPRESS

In this article, we extend this approach to ENZ materials and demonstrate that reflection from an ENZ layer can be effectively minimized and transmission through it maximized via a simple multilayer stack on top of the ENZ substrate. The AR coating is designed via the use of a Multi-Objective-Grey-Wolf-optimizer (MOGWO) [17], consists of commonly used materials, specifically silver (Ag) and silicon dioxide (SiO_2) and can be fabricated through simple electron beam evaporation of the materials.

2. Epsilon-near-zero substrate and fabrication techniques

As an ENZ material, we chose a metamaterial structure consisting of 5 bi-layers of 60 nm SiO_2 and 6 nm Ag, with half-thickness layers of SiO_2 at the top and bottom layer to ensure symmetry (and protection against oxidation of the Ag). The device is fabricated through electron beam evaporation of the materials, and each Ag layer incorporates a Germanium nucleation layer to ensure a smooth Ag film and avoid islanding [18].

This stack features an effective permittivity response which is characterized through transmission and reflection measurements. We use a nonlinear minimization optimizer combined with the Transfer Matrix Method (TMM) to find the effective permittivity that best reproduces the measurement data to infer the effective dispersion and ENZ spectral region of the ENZ-stack. The resulting effective dispersion can be found in Fig. 1. This result was then checked against an effective medium theory where the constituent layers' dispersions were measured via ellipsometry and the thicknesses of the layers inferred from SEM imaging were utilised in the calculation. The calculation suggested that the ENZ zero crossing point can be found between $\lambda = 650$ nm and $\lambda = 700$ nm, which is consistent with that retrieved from the TMM. We thus aim to optimize the optical transmission in this region.

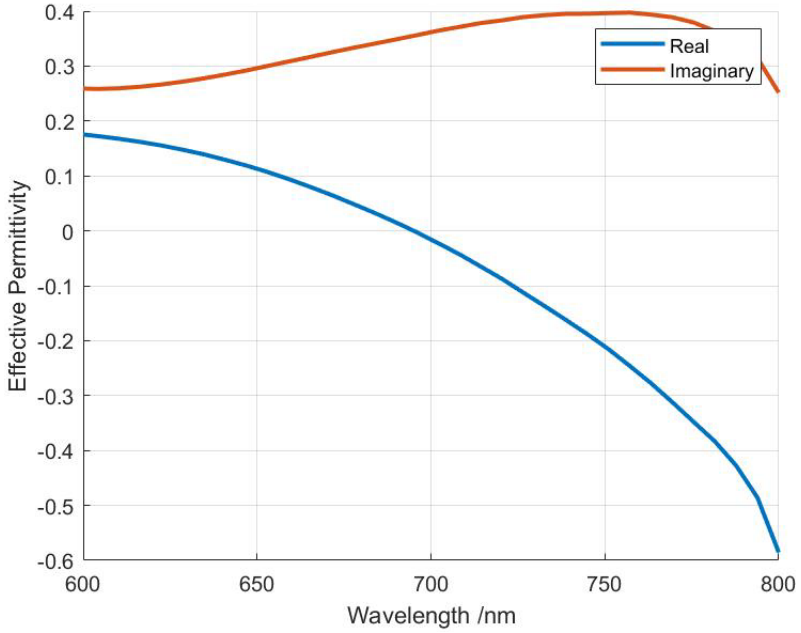

Fig. 1. Effective permittivity of the epsilon-near-zero multilayer retrieved via the transfer matrix method.

Optical Materials EXPRESS

3. Anti-reflection coating design

Before any optimisation or design of the AR coating can be performed we must choose and define appropriate figures of merit (FOM) to evaluate for the device. We note that previously other groups have used optimization algorithms to reduce the reflection from similar ENZ structures [19]. However, they have done so for the aim of creating a perfect absorber. As such, they had a simpler problem, as a large number of layers can be used, leading to strong optical losses. Here we want to enable a wide range of applications, including linear optical tasks such as wavefront shaping, where absorption is unwanted. Therefore, we do not optimize the reflection behaviour of the stack, but the transmission one. In our case, we perform optimisation over two FOM simultaneously. Specifically these are associated with the improvement in transmission at the ENZ-point and the bandwidth over which the transmission is enhanced. Thus the first FOM consists of the transmission through the metamaterial stack with the AR coating, T, normalized to that without an AR coating, T_0. This is then multiplied by a normal probability distribution centred on the ENZ wavelength, to give greater emphasis to improvements in the centre of the ENZ region, rather than at its edges. The figure of merit is given as follows:

$$FOM1 = \frac{1}{\sigma\sqrt{(2\pi)}} e^{\frac{-(x-\mu)^2}{2\sigma^2}} \frac{T}{T_0}. \tag{1}$$

Where σ is the standard deviation of the fitted normal distribution from the ENZ point and μ stands for the mean of the distribution. For our purposes, σ is given as 5, and μ is 650. The second figure of merit represents the AR-coating bandwidth and is obtained via a summation of the wavelengths at which an improvement is seen in T vs T_0.

$$sgn(\lambda) = \left\{ \begin{array}{ll} 1 & \text{if } T(\lambda) \geq T_0(\lambda) \\ 0 & \text{if } T(\lambda) < T_0(\lambda) \end{array} \right\} \tag{2}$$

$$FOM2 = \frac{1}{\sum_{\lambda_{min}}^{\lambda_{max}} sgn(\lambda) + 1} \tag{3}$$

The transmission at each wavelength for each member of the population is calculated using the TMM. The transmission, T_0, through the original metamaterial stack is also calculated via the TMM.

We perform the design of the AR-coating using a multi-objective optimisation algorithm. Specifically, we utilise a MATLAB implementation of the MOGWO as provided in Ref. [17]. Multi-objective optimizers yield a Pareto front [20], consisting of the non-dominated population. A non-dominated solution is one that is not outperformed with respect to both figures of merit simultaneously, i.e. if a solution is non-dominated, then no other solution has simultaneously a better transmission (FOM1) and bandwidth (FOM2), although other solutions might feature better values for one of these FOMs. The Pareto front thus demonstrates any compromise between the two figure of merits over which we optimize. Further details of how the optimizer functions and the parameters that were used for the optimisation given here can be found in Supplement 1.

Initially, to gauge what materials would be viable solutions for our multilayer design, we ran a series of runs where the wavelength range is restricted to a very narrow range of around 20nm around the ENZ zero-crossing point. The index of the materials are randomly generated between 0 and 6 for each layer and so are the thicknesses of the constituent layers. We found that optimizer, when run for 6,5,4 layer and 3 layer designs tended to having in-effect two layers of SiO_2 either side of a very high index medium as the ideal solution. Various high index semiconductors could serve as a substitute to metals like Ag in this high index layer. These would have lower losses than Ag as a material. We found that for candidates such as Germanium the losses were too

Optical Materials EXPRESS

high to yield an improvement, in part due to an increased film thickness compared to the Ag intermediate layer.

Once the materials to be used in the design were identified optimisations were run to optimize the thicknesses of the layers for a broad spectral range. We have three layers with SiO_2, Ag and SiO_2 as the constituent layers, the thicknesses of which constitute the randomly generated values of each member of the optimizer's population. These values were generated between 5 nm and 120 nm for the dielectric layers and the Ag could vary between 0 and 15 nm. The optimisation from which we find the solution that we fabricated only yields two possible solutions which are very similar to each other. Various options were applied to attempt to achieve the best Pareto front possible, but in this instance, there is a single solution which exceeds other candidates on both FOMS.

The values and materials utilised in the final design that we fabricated can be found in Table 1.

Table 1. Structure of design that was fabricated and designed to yield high transmission and minimal reflection.

Layer	Material	Thickness/nm
1	SiO_2	120
2	Ag	8
3	SiO_2	103
Original Meta-material Stack	-	-

4. Experimental verification of AR coating design

The solution shown in Table 1 was fabricated in the same manner as the ENZ-metamaterial. Simultaneously we fabricated a reference sample, consisting of the underlying ENZ metamaterial, without the AR coating, to eliminate the effects of run-to-run variations in device fabrication. An SEM image of the constituent layers of the multi-layer can be found in Fig. 2. The transmission and reflection of both samples were determined using the experimental set up shown in Fig. 3.

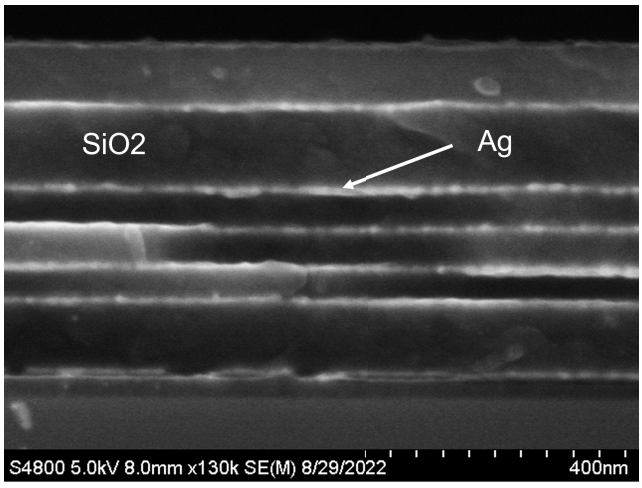

Fig. 2. SEM cross-section of the cleaved multi layer on a Si substrate which shows the constituent layers

The light from a broadband halogen lamp is collimated and then directed onto the sample at normal incidence. The reflected and transmitted light are collected via a multi-mode fibre and

Optical Materials EXPRESS

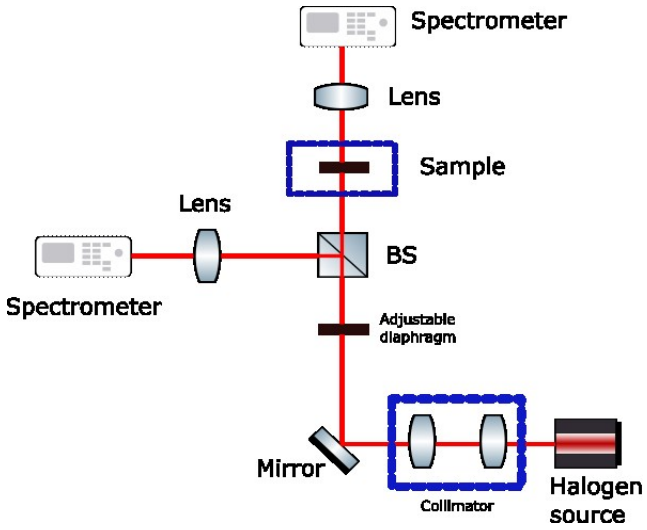

Fig. 3. A diagram of the experimental setup used to characterize multi-layers in the visible range , containing a halogen source, collimation section and diaphragm, sample and spectrometers

sent to an Ocean Optics spectrometer. The measured data is shown in Fig. 4. Further details concerning the experimental method can be found in Ref. [21].

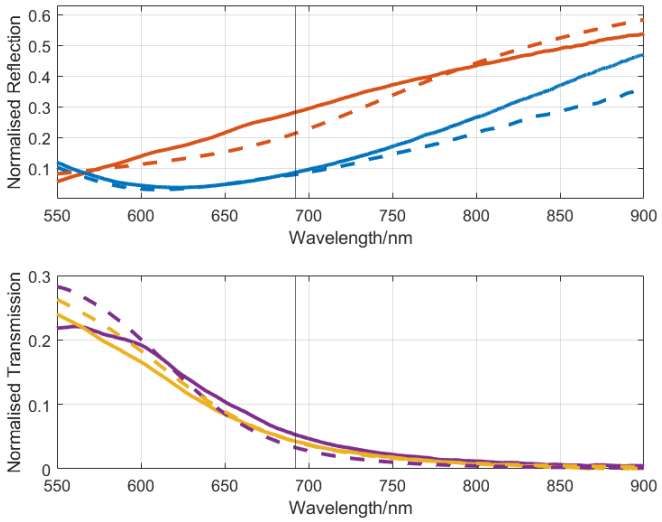

Fig. 4. Top: Experimental measurement of the reflection through the original metamaterial slab(orange) and coated metamaterial slab (blue) combined with the TMM calculation (dashed lines). Bottom: Experimental measurement of the transmission through both metamaterial slabs both coated (purple) and uncoated (yellow) combined with the TMM calculation (dashed lines).

The experimental data shown in Fig. 5 confirms that the AR coating enhances the transmission in the ENZ region, with the transmission improving by around 20% over a bandwidth of 150 nm. Simultaneously, the reflectivity is reduced over a range of 200nm by approximately 50% or

Optical Materials EXPRESS

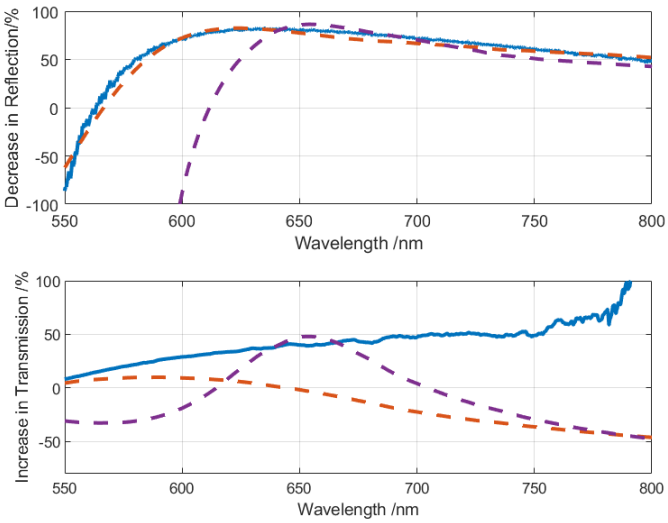

Fig. 5. Top: Blue line is the improvement in reflection from experimental data, Dashed Orange line is the percentage decrease given by the TMM model, Dashed Purple line is the ideal result given from the original optimisation. Bottom: Blue line is the experimental measurement of the increase in transmission, the dashed orange line is the prediction from the TMM model for the fabricated multilayer, the dashed purple line is the ideal solution as given by the optimisation.

more. We provide TMM data for the fabricated metamaterial stack where the dielectric layer thicknesses have been inferred from SEM imaging of the meta-material cross-section. The TMM calculated using the original parameters used in the initial optimisation yields over a 40 percent improvement in transmission meanwhile, the result for the fabricated design does not show the desired improvement in the region of interest. These differences can be attributed to experimental uncertainties, such as variations in the thickness of the layers across the sample and potential variations in the Ag dispersion. For thin films of metals, the film quality, including conductivity and therefore optical dispersion, is strongly dependent on the film thickness and deposition process [22,23], even in the presence of the Ge nucleation layer. As such, the dispersion of the 8 nm layer in the AR coating will differ slightly from that of the 6 nm Ag film in the ENZ section of the multi-layer stack. However, during the optimisation process, the Ag dispersion was taken to be constant over the thickness range investigated (for simplicity).

We note that the coated stack has an additional bi-layer with a different filling fraction to the original structure and hence light is not scattered in the periodic manner as before which breaks the EMT approximation. There is also the additional factor that the coated multi-layer in its entirety is 561nm thick meaning that the structures dimensions are around a wavelength thick for some of the measurement range hence etalon behaviour can occur which also breaks the EMT approximation. The light which is transmitted through the sample propagates through the additional sub-wavelength structuring, and hence the point of zero-phase propagation is slightly different to that of the initial stack.

Finally, we note that in our work the AR coating was only used on one interface, specifically the ENZ-air interface. A similar coating could be designed for the ENZ-substrate interfaces, leading to further improvements in the device transmission, as this interface still features a high impedance mismatch in our work.

Optical Materials EXPRESS

5. Conclusion

We demonstrate a simple AR coating for ENZ metamaterials that enhances transmission through the metamaterial by 20% over 150 nm bandwidth. This performance could be further improved through an additional AR coating on the bottom of the ENZ layer, i.e. at the ENZ substrate interface. The coating consists of 2 layers of SiO_2 and one layer of Ag, the same materials used in the underlying ENZ stack and can be fabricated in the same evaporation step. Thus no additional fabrication complexity is introduced. This AR coating has the potential to improve the performance of all applications based on ENZ-multilayer stacks and is also compatible with conformal fabrication approaches [24].

Funding. Engineering and Physical Sciences Research Council (EP/N509759/1, EP/R513337/1); European Research Council (ERC) under the European Union Horizon 2020 Research and Innovation Program (819346).

Acknowledgments. ADF acknowledges support from the European Research Council (ERC) under the European Union Horizon 2020 research and innovation program (Grant Agreement No. 819346).

Disclosures. The authors declare that there are no conflicts of interest related to this article.

Data availability. Data underlying the results presented in this paper are available in Ref. [25].

Supplemental document. See Supplement 1 for supporting content.

References

1. O. Reshef, I. De Leon, M. Z. Alam, and R. W. Boyd, "Nonlinear optical effects in epsilon-near-zero media," Nat. Rev. Mater. **4**(8), 535–551 (2019).
2. M. A. Vincenti, D. de Ceglia, and M. Scalora, "Enz materials and anisotropy: enhancing nonlinear optical interactions at the nanoscale," Opt. Express **28**(21), 31180–31196 (2020).
3. M. Z. Alam, I. D. Leon, and R. W. Boyd, "Large optical nonlinearity of indium tin oxide in its epsilon-near-zero region," Science **352**(6287), 795–797 (2016).
4. D. A. Powell, A. Alù, B. Edwards, A. Vakil, Y. S. Kivshar, and N. Engheta, "Nonlinear control of tunneling through an epsilon-near-zero channel," Phys. Rev. B **79**(24), 245135 (2009).
5. J. R. Gagnon, O. Reshef, D. H. G. Espinosa, M. Z. Alam, D. I. Vulis, E. N. Knall, J. Upham, Y. Li, K. Dolgaleva, E. Mazur, and R. W. Boyd, "Relaxed phase-matching constraints in zero-index waveguides," Phys. Rev. Lett. **128**(20), 203902 (2022).
6. O. Reshef, Y. Li, M. Yin, L. Christakis, D. I. Vulis, P. C.-M. noz, S. Kita, M. Lonicar, and E. Mazur, "Phase-matching in dirac-cone-based zero-index metamaterials," in *Conference on Lasers and Electro-Optics*, (Optica Publishing Group, 2016), p. JTu5A.53.
7. G. Briere, B. Cluzel, and O. Demichel, "Improving the transmittance of an epsilon-near-zero-based wavefront shaper," Opt. Lett. **41**(19), 4542–4545 (2016).
8. H. Hajian, E. Ozbay, and H. Caglayan, "Beaming and enhanced transmission through a subwavelength aperture via epsilon-near-zero media," Sci. Rep. **7**(1), 4741 (2017).
9. J. Luo and Y. Lai, "Anisotropic zero-index waveguide with arbitrary shapes," Sci. Rep. **4**(1), 5875 (2014).
10. J. Kim, E. G. Carnemolla, C. DeVault, A. M. Shaltout, D. Faccio, V. M. Shalaev, A. V. Kildishev, M. Ferrera, and A. Boltasseva, "Dynamic control of nanocavities with tunable metal oxides," Nano Lett. **18**(2), 740–746 (2018).
11. X. Niu, X. Hu, S. Chu, and Q. Gong, "Epsilon-near-zero photonics: A new platform for integrated devices," Adv. Opt. Mater. **6**(10), 1701292 (2018).
12. R. M. Kaipurath, M. Pietrzyk, L. Caspani, T. Roger, M. Clerici, C. Rizza, A. Ciattoni, A. Di Falco, and D. Faccio, "Optically induced metal-to-dielectric transition in epsilon-near-zero metamaterials," Sci. Rep. **6**(1), 27700 (2016).
13. E. J. R. Vesseur, T. Coenen, H. Caglayan, N. Engheta, and A. Polman, "Experimental verification of n= 0 structures for visible light," Phys. Rev. Lett. **110**(1), 013902 (2013).
14. M. Z. Alam, S. A. Schulz, J. Upham, I. De Leon, and R. W. Boyd, "Large optical nonlinearity of nanoantennas coupled to an epsilon-near-zero material," Nat. Photonics **12**(2), 79–83 (2018).
15. S. A. Schulz, A. A. Tahir, M. Z. Alam, J. Upham, I. De Leon, and R. W. Boyd, "Optical response of dipole antennas on an epsilon-near-zero substrate," Phys. Rev. A **93**(6), 063846 (2016).
16. C. A. Riedel, K. Sun, O. L. Muskens, and C. de Groot, "Nanoscale modeling of electro-plasmonic tunable devices for modulators and metasurfaces," Opt. Express **25**(9), 10031–10043 (2017).
17. S. Mirjalili, S. Saremi, S. M. Mirjalili, and L. dos S. Coelho, "Multi-objective grey wolf optimizer: A novel algorithm for multi-criterion optimization," Expert Systems with Applications **47**, 106–119 (2016).
18. L. V. J. N. P. Kobayashi, M. S. Islam, W. Wu, P. Chaturvedi, N. X. Fang, S. Y. Wang, and R. S. Williams, "Ultrasmooth silver thin films deposited with a germanium nucleation layer," Nano Lett. **9**(1), 178–182 (2009).
19. J. Yoon, M. Zhou, M. A. Badsha, T. Y. Kim, Y. C. Jun, and C. K. Hwangbo, "Broadband epsilon-near-zero perfect absorption in the near-infrared," Sci. Rep. **5**(1), 12788 (2015).

Optical Materials EXPRESS

20. K. Deb, A. Pratap, S. Agarwal, and T. Meyarivan, "A fast and elitist multiobjective genetic algorithm: NSGA-II," IEEE Transactions on Evol. Comput. **6**(2), 182–197 (2002).
21. M. Pietrzyk, R. Kaipurath, D. Faccio, and A. Di Falco, "Epsilon near zero metamaterials for ultra-low power nonlinear applications," in *Photonic and Phononic Properties of Engineered Nanostructures V*, vol. 9371 (SPIE, 2015), pp. 48–53.
22. H. C. Kim, N. D. Theodore, and T. L. Alford, "Comparison of texture evolution in Ag and Ag(Al) alloy thin films on amorphous SiO_2," J. Appl. Phys. **95**(9), 5180–5188 (2004).
23. S. Laref, J. Cao, A. Asaduzzaman, K. Runge, P. Deymier, R. W. Ziolkowski, M. Miyawaki, and K. Muralidharan, "Size-dependent permittivity and intrinsic optical anisotropy of nanometric gold thin films: a density functional theory study," Opt. Express **21**(10), 11827–11838 (2013).
24. X. Li, C. Rizza, S. A. Schulz, A. Ciattoni, and A. Di Falco, "Conformable optical coatings with epsilon near zero response," APL Photonics **4**(5), 056107 (2019).
25. L. Wynne, C. Zhang, B. Akpan, A. Di Falco, and S. Schulz, "Anti-reflection coating for epsilon-near-zero materials (dataset)," University of St Andrews Research Portal 2022, https://doi.org/10.17630/4c22ccc6-da47-4c74-8429-7a30b7b30aa6.